The International Journal of Cardiovascular Imaging (2019) 35:733–739
https://doi.org/10.1007/s10554-018-1499-6

ORIGINAL PAPER

Coronary artery calcium scoring with photon-counting CT: first in vivo human experience

Rolf Symons[1,2] · Veit Sandfort[1] · Marissa Mallek[1] · Stefan Ulzheimer[3] · Amir Pourmorteza[1,4,5]

Received: 13 August 2018 / Accepted: 7 November 2018 / Published online: 11 January 2019

Abstract

To evaluate the performance of photon-counting detector (PCD) computed tomography (CT) for coronary artery calcium (CAC) score imaging at standard and reduced radiation doses compared to conventional energy-integrating detector (EID) CT. A dedicated cardiac CT phantom, ten ex vivo human hearts, and ten asymptomatic volunteers underwent matched EID and PCD CT scans at different dose settings without ECG gating. CAC score, contrast, and contrast-to-noise ratio (CNR) were calculated in the cardiac CT phantom. CAC score accuracy and reproducibility was assessed in the ex vivo hearts. Standard radiation dose (120 kVp, reference mAs = 80) in vivo CAC scans were compared against dose-reduced CAC scans (75% dose reduction; reference mAs = 20) for image quality and CAC score reproducibility. Interstudy agreement was assessed by using intraclass correlation (ICC), linear regression, and Bland–Altman analysis with 95% confidence interval limits of agreement (LOA). Calcium-soft tissue contrast and CNR were significantly higher for the PCD CAC scans in the cardiac CT phantom (all $P < 0.01$). Ex vivo hearts: CAC score reproducibility was significantly higher for the PCD scans at the lowest dose setting (50 mAs) ($P = 0.002$); score accuracy was similar for both detector systems at all dose settings. In vivo scans: the agreement between standard dose and low dose CAC score was significantly better for the PCD than for the EID with narrower LOA in Bland–Altman analysis, linear regression slopes closer to 1 (0.96 vs. 0.84), and higher ICC values (0.98 vs. 0.93, respectively). Phantom and in vivo human studies showed PCD may significantly improve CAC score image quality and/or reduce CAC score radiation dose while maintaining diagnostic image quality.

Keywords Coronary artery calcium score · Photon-counting CT · Radiation dose reduction

Introduction

Coronary artery calcium (CAC) score has been validated as an independent predictor of cardiovascular events and has been proposed as a screening tool for coronary artery disease (CAD) in asymptomatic subjects as part of a comprehensive risk assessment [1, 2]. However, the benefits of screening have to be assessed against the inherent risks of exposing asymptomatic individuals to ionizing radiation [3]. Accordingly, multiple technical advances are being investigated to reduce the radiation dose of CAC screening, including prospectively gated scanning and iterative reconstruction algorithms [4].

Photon-counting detectors (PCDs) are a novel CT detector technology which may have substantial benefits for CAC score imaging [5, 6]. Contrary to conventional energy-integrating detectors (EIDs) which combine the electrical signal of multiple X-ray photons into a single intensity value, PCDs

Rolf Symons and Veit Sandfort contributed equally to this manuscript.

✉ Amir Pourmorteza
amir.pourmorteza@emory.edu

1 Radiology and Imaging Sciences - National Institutes of Health Clinical Center, Bethesda, MD, USA

2 Department of Imaging & Pathology, University Hospitals Leuven, Leuven, Belgium

3 Siemens Healthcare GmbH, Forchheim, Germany

4 Department of Radiology and Imaging Sciences, Emory University School of Medicine, Atlanta, GA, USA

5 Department of Radiology and Imaging Sciences, Winship Cancer Institute of Emory University, 1701 Uppergate Drive, Suite 5018A, Atlanta, GA 30322, USA

can measure the number and energy of individual X-ray photons. PCD CT scan have been shown to improve tissue contrast, Hounsfield unit (HU) stability, and suppress electronic noise, and reduce noise-aliasing, all of which contribute to increase in CT contrast-to-noise ratios (CNR) and allow for significant reductions in radiation dose exposure while maintaining diagnostic quality [7–12]. The aim of this study was to assess the performance of a prototype PCD scanner for CAC score at standard and low radiation doses and to compare the results with state-of-the-art EID technology.

Materials and methods

Study design

This institutional review board-approved study with informed consent prospectively enrolled ten asymptomatic volunteers older than 45 years [5 male, mean age ± standard deviation (SD): 58 ± 10 years] at the National Institutes of Healt (NIH) Clinical Center. Exclusion criteria included pregnancy, prior CT scan within the previous 12 months, and genetic predisposition to radiation-induced cancer.

Phantom studies

A commercially available cardiac CT phantom (QRM Cardio phantom, QRM GmbH, Mohrendorf, Germany) developed for testing reproducibility in CAC scans [13] was used (Fig. 1). The phantom contains nine cylindrical hydroxyapatite (HA) inserts of varying size (5.0, 3.0, and 1.0 mm) and density (200, 400, and 800 mg/ml of HA) simulating the range of calcifications typically seen in CAC scans. The calcifications are embedded in a soft tissue-equivalent plastic (35 HU at 120 kVp). Additionally, ten ex vivo human hearts were studied at multiple dose settings. All subjects signed informed consent to donate their organs to science for research purposes. The hearts were fixed in formaldehyde and placed in a ring-shaped phantom of water-equivalent material (QRM GmbH, Mohrendorf, Germany) for CAC imaging (Fig. 2). The inner and outer diameter of the ring phantom were 100 mm and 200 mm, respectively.

Photon-counting CT scanner

The prototype CT scanner used in this work is a modified version of a commercially available dual-source scanner (SOMATOM Definition Flash; Siemens Healthcare, Forchheim, Germany). The scanner has two independent X-ray source-detector subsystems that are 95° apart. One of the two EIDs in the scanner is replaced with a cadmium-telluride PCD. The detailed specifications of the scanner have been previously reported [8, 14]. This set-up with identical X-ray tubes, beam-shaping filters, and scanner geometry provides a suitable platform for direct comparison of the two detector technologies. The EID and PCD subsystems have field-of-view (FOV) of 500 mm and 275 mm, and a collimation × pixel pitch of 64 × 0.6 mm and 32 × 0.5 mm at isocenter, respectively. Each PCD pixel consists of 4 × 4 subpixels, each with two adjustable photon energy detection thresholds. The lower and higher thresholds can be set between 20–50 and 50–90 keV, respectively. We set the lower threshold at 22 keV. Since evaluating the spectral performance of PCD at low radiation dose was outside the scope of this study, the high threshold was arbitrarily set at 75 keV. We reconstructed PCD images from photons detected in the 22–120 keV energy range.

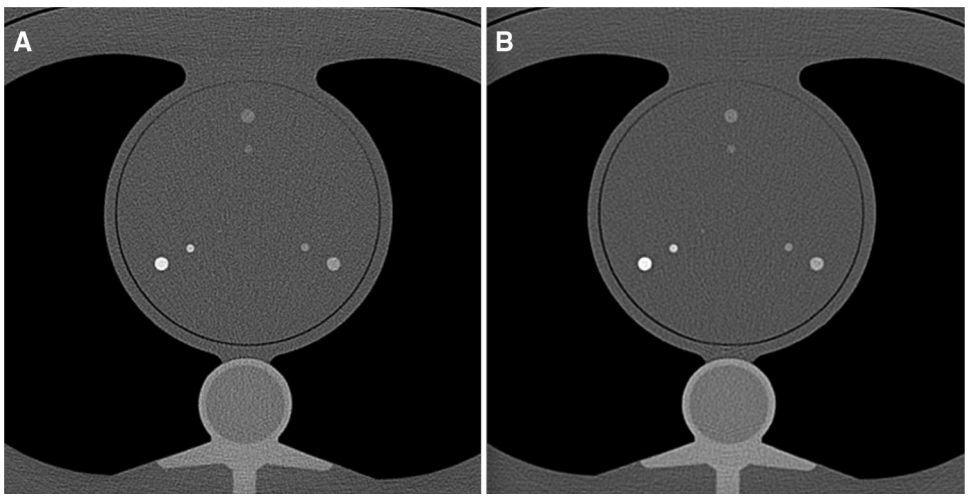

Fig. 1 Sample energy-integrating detector (EID) (**a**) and photon-counting detector (PCD) (**b**) scans of the QRM cardiac phantom. The phantom contains 3 × 3 cylindrical hydroxyapatite (HA) calcifications of varying size (5.0, 3.0, and 1.0 mm) and density (200, 400, and 800 mg/ml of HA) simulating the range of calcifications typically seen in CAC scans. The calcifications are embedded in a soft tissue-equivalent plastic (35 HU at 120 kVp)

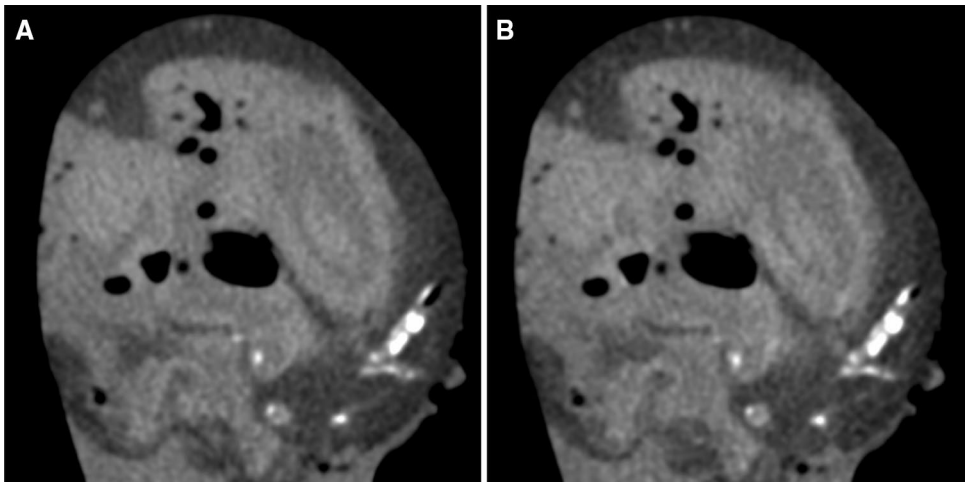

Fig. 2 Sample energy-integrating detector (EID) (**a**) and photon-counting detector (PCD) (**b**) scans of an ex vivo heart demonstrate extensive coronary calcifications in the left anterior descending artery (LAD)

Image acquisition and reconstruction

Volunteer scans

CAC score scans were performed at clinical routine settings [tube voltage: 120 kVp, reference tube current–time product: 80 mAs for a typical 75-kg subject adapted to individual patient size by using vendor-supplied software (Caredose4D, Siemens Healthcare)]. Additionally, low dose CAC scans were acquired at 75% dose reduction (tube voltage: 120 kVp, reference tube current–time product: 20 mAs for a typical 75-kg subject). Each EID CAC scan was followed by a PCD scan with matched tube voltage and current settings after a 5–10-s delay for breath-hold instructions. We used the standard dose EID CAC score as our clinical reference. No cardiac gating was used as it was not yet available on the prototype system, therefore a relatively high pitch factor of 1.5 was used to speed up the acquisition.

Phantom and ex vivo studies

QRM phantom scans were performed at the same settings as the human scans. The human ex vivo hearts were scanned at multiple dose settings (tube voltage: 120 kVp, reference tube current–time product: 500, 140, 80, and 50 mAs). Each acquisition was repeated five times to assess reproducibility. All images were reconstructed using weighted filtered backprojection (FBP) (ReconCT v.13.8.5.0, Siemens Healthcare) with 3-mm slice thickness, 3-mm increment, 512 × 512 matrix, and a soft tissue kernel optimized for CAC score (B35f).

Image analysis

CAC score contrast and CNR were calculated as $contrast_{CAC} = \mu_{Ca} - \mu_{soft\ tissue}$ and $CNR_{CAC} = (\mu_{Ca} - \mu_{soft\ tissue})/\sigma_{soft\ tissue}$, respectively, by drawing regions-of-interest (ROIs) in the calcifications and soft tissue-equivalent materials of the QRM cardio phantom. Only the largest 5.0 mm diameter calcifications were used to avoid partial volume effects. The reproducibility of CAC scores at different dose levels was evaluated by evaluating the SD of the ex vivo heart CAC scores measured at each mAs setting. The accuracy of CAC scores at different dose levels was evaluated by using the sum of squared errors with the mean CAC score of the five ex vivo heart acquisition repetitions at the highest dose setting as reference. CAC score analysis was performed on the ex vivo hearts and human subjects using commercially available software (Vitrea, Vital images, Minnetonka, MN, USA) by a cardiologist with > 5 years of experience in analyzing cardiac CT images. Each coronary artery [right coronary artery (RCA), left anterior descending artery (LAD), and left circumflex artery (LCx)] was scored individually. Additionally, calcifications of the ascending and descending aorta were measured. Motion artifacts were assessed on a qualitative scale (0 = no motion artifacts; 1 = mild motion artifacts; 2 = moderate motion artifacts; 3 = severe motion artifacts). CAC scores were reanalyzed after 4 weeks to assess reader reproducibility. Image noise was defined as the SD of a > 1 cm^2 ROI placed in the left ventricle (LV) blood pool (OsiriX, Pixmeo, Geneva, Switzerland). For Agatston CAC score, only voxels with density > 130 HU are counted. Therefore, noise-induced HU values above this threshold may be mistaken for coronary calcium. Therefore, as a measure of CAC score robustness, we measured the number of voxels with a density > 130 HU in a 3D ROI without calcium (LV blood pool).

Statistical analysis

R statistical software (v.3.4.0, Foundation for Statistical Computing, Vienna, Austria) was used for statistical analysis. The Shapiro–Wilk test was used to assess normality of the data distributions. Continuous variables were expressed as mean ± SD or median with interquartile

ranges (IQR), as appropriate. The paired *t* test or Wilcoxon rank test was used to compare groups, as appropriate. Interstudy agreement between standard and low dose CAC score scans was assessed by using intraclass correlation (ICC) (strong agreement: ICC > 0.75, moderate agreement: ICC = 0.40–0.75, poor agreement: ICC < 0.40), linear regression, and Bland–Altman analysis with 95% confidence interval (CI) limits of agreement (LOA) [15]. The difference between ICCs was considered to be statistically significant when there was no overlap between their respective 95% CI limits. P value < 0.05 was considered to indicate statistical significance.

Results

Average tube current–time product and $CTDI_{vol}$ were 23 mAs (range 14–32 mAs) and 1.6 mGy (range 0.9–2.2 mGy) for low-dose CAC and 79 mAs (range 38–124 mAs) and 5.4 mGy (range 2.6–8.4 mGy) for standard dose CAC, respectively. No subjects were excluded from analysis after enrollment.

Phantom calcium-soft tissue contrast and CNR

Calcium inserts attenuation values, contrast, and CNR values are summarized in Table 1. PCD calcium attenuation values were significantly higher than EID values for all calcium insert densities (all P < 0.01), whereas PCD soft tissue values were only slightly higher than EID values (42.5 ± 5.2 HU and 36.8 ± 1.4 HU, P = 0.02). This resulted in significantly higher calcium—soft tissue contrast and CNR for the PCD scans (all P < 0.01).

CAC score reproducibility and accuracy in ex vivo hearts

CAC score reproducibility was significantly higher for the PCD scans at the lowest dose setting [median SD of CAC scores: 13.5 (IQR: 10.7–14.2) vs. 18.5 (IQR: 17.8–28.1) for PCD and EID, respectively, P = 0.002]. CAC score accuracy (using the 500 mAs high dose scans of each detector as reference) was similar for both detector systems at all dose settings (Fig. 3).

In vivo low dose CAC score

The mean age was 58 ± 10 years (five male, five female, heart rate 65 ± 7 beats per minute). No significant bias was observed between standard dose EID CAC scores and low dose EID or low dose PCD CAC scores in Bland–Altman analysis (bias: − 24.8, 95% LOAs: − 85.6, 36.0 and bias: − 10.8, 95% LOAs: − 52.0, 30.4, respectively) (Fig. 4). However, the agreement between standard dose and low dose CAC score was significantly better for the PCD than for the EID scans with narrower LOA in Bland–Altman analysis and higher ICC values (ICC: 0.98, 95% CI 0.97–0.99 and ICC: 0.93, 95% CI 0.88–0.95, respectively). Linear regression analysis showed a slope of 0.96 for low dose PCD CAC scores when compared to standard dose EID, indicating excellent linear reliability. Conversely, low dose EID CAC scores showed a slope of 0.84, indicating a tendency to underestimate CAC scores when compared to standard dose EID. Reader reproducibility for CAC scores was excellent (ICC: 0.99, 95% CI 0.991–0.993). No differences were found between men and women.

In vivo image quality

Noise levels were similar between EID and PCD CAC scans both at standard and at low dose settings (18.7 ± 3.5 HU vs. 18.0 ± 2.8 HU and 34.3 ± 4.5 HU vs. 32.9 ± 4.0

Table 1 Image quality comparison between conventional energy-integrating detector (EID) and photon-counting detector (PCD) scans in the QRM cardiac phantom

Measurement	Detector	Calcium insert			Soft tissue
		800 HA	400 HA	200 HA	
Attenuation value (HU)	EID	909.3 ± 5.1	431.8 ± 7.1	238.7 ± 5.5	42.5 ± 2.2
	PCD	1052.4 ± 4.6	522.0 ± 4.9	260.5 ± 6.7	36.8 ± 1.4
	P value	< 0.001	< 0.001	0.003	0.02
Contrast (HU)	EID	866.8 ± 4.4	389.3 ± 5.3	196.2 ± 4.8	–
	PCD	1015.6 ± 5.1	485.2 ± 4.5	223.7 ± 6.9	–
	P value	< 0.001	< 0.001	0.002	
CNR	EID	19.7 ± 0.2	8.9 ± 0.1	4.5 ± 0.1	–
	PCD	22.7 ± 0.1	10.9 ± 0.1	5.0 ± 0.2	–
	P value	< 0.001	< 0.001	0.005	

CNR contrast-to-noise ratio, *HU* Hounsfield unit

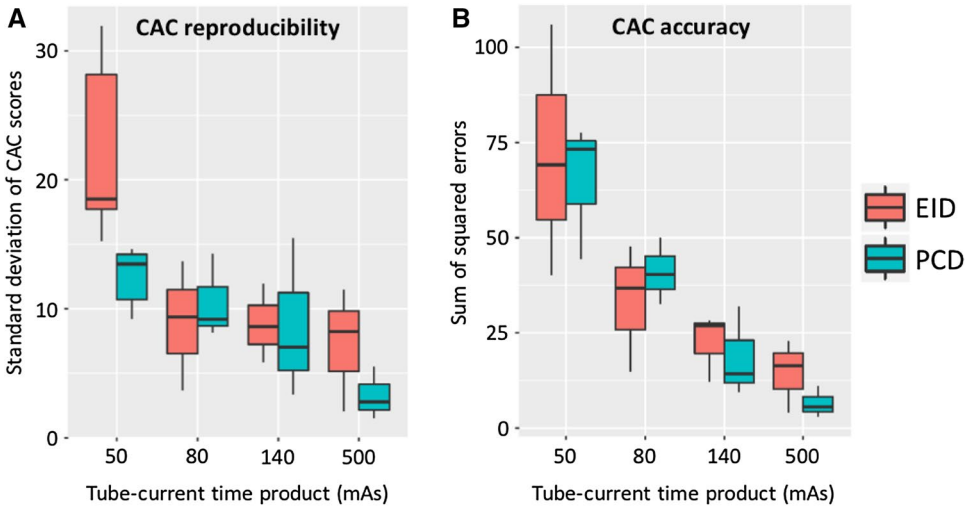

Fig. 3 CAC score reproducibility (**a**) and CAC score accuracy (**b**) measured in ten ex vivo human hearts, with five repeated EID and PCD scans at each mAs setting. At the lowest dose setting (50 mAs) CAC score reproducibility was significantly higher for the PCD scans (P = 0.002), whereas CAC score accuracy was similar for both detector systems at all dose settings

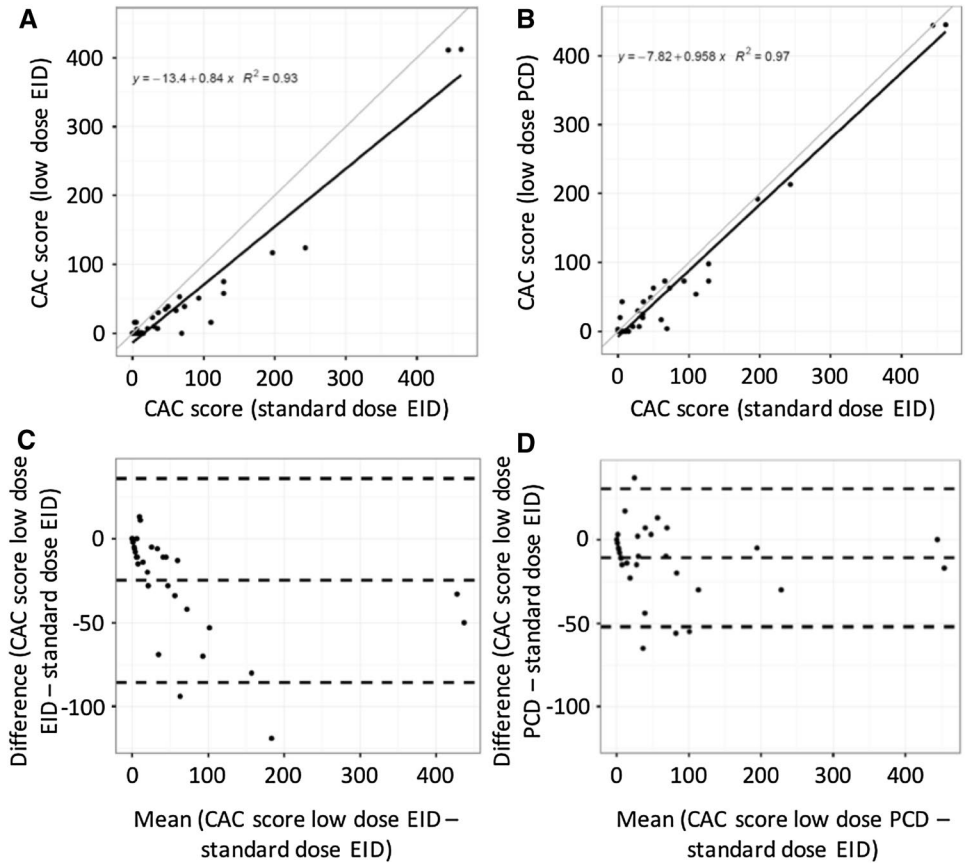

Fig. 4 Low dose performance of photon-counting CT: linear regression plots (**a, b**) showed a slope of 0.96 for low dose PCD CAC scores when compared to standard dose EID (**b**), indicating excellent linear reliability. Conversely, low dose EID CAC scores showed a slope of 0.84, indicating a tendency to underestimate CAC scores when compared to standard dose EID (**a**). Bland–Altman analysis (**c, d**) showed no significant bias between standard dose EID CAC scores and low dose EID or PCD CAC scores. However, reproducibility of low dose PCD CAC scores was better with smaller limits of agreement (**d**)

HU, respectively). However, the average number of voxels with a density of > 130 HU was slightly higher for low dose EID images than low dose PCD images (177.4 vs. 125.2, P < 0.05). Qualitative assessment of motion artifacts showed no significant difference between EID and PCD scans (1.3 ± 1.0 and 1.4 ± 0.9, respectively) (Fig. 5).

Discussion

We hypothesized the improved tissue contrast, HU stability, and suppression of electronic noise of photon-counting CT detector technology may improve quality of CAC score

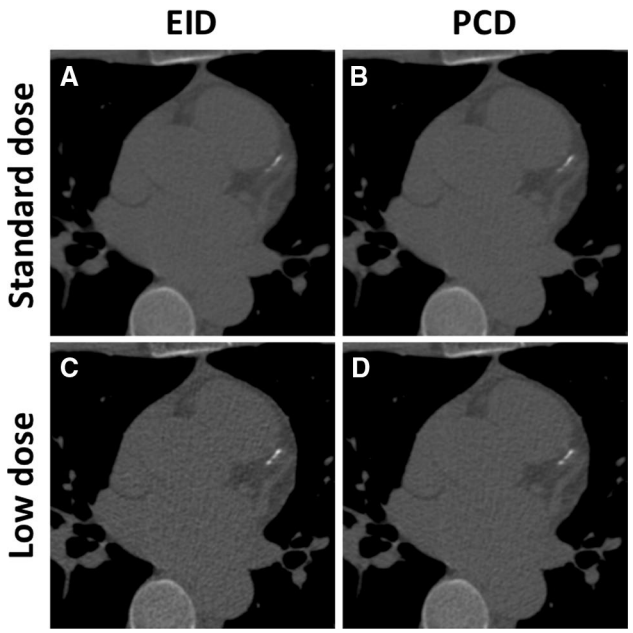

Fig. 5 Sample energy-integrating detector (EID) (**a, c**) and photon-counting detector (PCD) (**b, d**) scans of a 67-year-old man at standard (**a, b**) and low (**c, d**) radiation dose (window center: 300, window width: 1500) show multiple adjacent calcified plaques on the left anterior descending (LAD) artery. At low radiation dose, the reproducibility of EID CAC scores was lower

scans. Our results indicated superior calcium-soft tissue contrast for PCD CAC scans with better low dose CAC score reproducibility and a smaller number of voxels above the Agatston threshold of > 130 HU (i.e. false positives) compared to the EID low dose CAC scans.

Simulations and phantom studies have shown the potential benefits of PCD for calcium imaging [16]. First, PCD calcium attenuation values at 120 kVp are higher than those of EID scans due to the better weighting of low-energy photons which carry more soft tissue contrast [5, 10]. The resulting increase in calcium versus soft tissue contrast may explain the observed higher reproducibility of PCD CAC scores at low dose in vivo. Second, the improved HU stability and lower susceptibility to electronic noise of PCD at low radiation doses strengthen the reliability of CAC scores at low radiation doses [8–10]. Finally, the potential introduction of high-resolution CAC scores imaging with PCD may not only lead to the detection of smaller calcified coronary lesions, but also further reduce radiation doses by the better sampling of high-frequency noise and reduced noise aliasing [12, 17].

Our results suggest PCD technology may play a role in reducing CAC score radiation doses. This is of particular importance as technological advances have dramatically reduced the radiation dose of coronary CT angiography (CCTA) from > 15 to < 1 mSv in select patients with good reproducibility making serial CCTA with CAC score clinically feasible for non-invasive longitudinal coronary plaque follow [18–20]. These technological advances include prospective electrocardiographically gated spiral scan modes, low tube voltage scanning, iterative reconstruction techniques, and single heartbeat scans using wide-detectors or dual-source systems with high pitch modes. However, the radiation dose reductions in CAC score imaging have been far less dramatic with CAC score now representing up to 50% of the total radiation dose of a CCTA study [21]. Our results suggest the superior performance of PCD technology at low radiation doses and the improved calcium—soft tissue contrast may play a complementary role to other radiation dose reducing techniques such as iterative reconstruction to further reduce the radiation dose of CAC scans [22, 23].

Some study limitations should be mentioned. First, the PCD prototype scanner used in this study is an investigational device. No US Food and Drug Administration approved PCD scanner is commercially available at the time of this study. Second, ECG gating was not available yet on the PCD prototype system. However, motion artifacts were rather limited for in vivo CAC scores and comparable between both detector systems. Nevertheless, future studies with ECG-gated CAC scoring are warranted to confirm our findings. Third, we opted to use FBP to avoid any bias or non-linearities in our reconstruction and allow for the fairest comparison between the two detector technologies. However, further studies have to confirm the superiority of PCD technology with the use of iterative reconstruction algorithms which can further reduce CAC score radiation doses [23]. Finally, PCD technology may have additional substantial benefits for CAC score and CCTA such as high-resolution imaging [24] and spectral material decomposition [25–31], which were beyond the scope of this study.

In conclusion, our phantom and in vivo human studies demonstrated the potential of PCD technology to improve CAC score image quality and/or to reduce radiation dose while maintaining diagnostic image quality.

Funding This study was supported by the NIH intramural research program (ZIACL090019; ZIAEB000072), and a collaborative research agreement with Siemens Healthcare GmbH (Forchheim, Germany).

Compliance with ethical standards

Conflict of interest None.

References

1. Detrano R, Guerci AD, Carr JJ et al (2008) Coronary calcium as a predictor of coronary events in four racial or ethnic groups. N Engl J Med 358:1336–1345

2. Greenland P, LaBree L, Azen SP et al (2004) Coronary artery calcium score combined with Framingham score for risk prediction in asymptomatic individuals. JAMA 291:210–215
3. Kim KP, Einstein AJ, de González AB (2009) Coronary artery calcification screening: estimated radiation dose and cancer risk. Arch Intern Med 169:1188–1194
4. Yin W-H, Lu B, Hou Z-H et al (2013) Detection of coronary artery stenosis with sub-milliSievert radiation dose by prospectively ECG-triggered high-pitch spiral CT angiography and iterative reconstruction. Eur Radiol 23:2927–2933
5. Taguchi K, Iwanczyk JS (2013) Vision 20/20: single photon counting X-ray detectors in medical imaging. Med Phys. https://doi.org/10.1118/1.4820371
6. Willemink MJ, Persson M, Pourmorteza A et al (2018) Photon-counting CT: technical principles and clinical prospects. Radiology 289:293–312
7. Gutjahr R, Halaweish AF, Yu Z et al (2016) Human imaging with photon counting-based computed tomography at clinical dose levels: contrast-to-noise ratio and cadaver studies. Investig Radiol 51:421–429
8. Symons R, Cork TE, Sahbaee P et al (2016) Low-dose lung cancer screening with photon-counting CT: a feasibility study. Phys Med Biol 62:202
9. Symons R, Pourmorteza A, Sandfort V et al (2017) Feasibility of dose-reduced chest CT with photon-counting detectors: initial results in humans. Radiology 285:980–989
10. Pourmorteza A, Symons R, Reich DS et al (2017) Photon-counting CT of the brain: in vivo human results and image-quality assessment. Am J Neuroradiol 38:2257–2263
11. Symons R, Reich DS, Bagheri M et al (2018) Photon-counting computed tomography for vascular imaging of the head and neck: first in vivo human results. Investig Radiol. https://doi.org/10.1097/RLI.0000000000000418
12. Pourmorteza A, Symons R, Schoek F et al (2018) Dose efficiency of quarter-millimeter photon-counting CT: first-in-human results. Investig Radiol 53:365–372
13. Ulzheimer S, Kalender WA (2003) Assessment of calcium scoring performance in cardiac computed tomography. Eur Radiol 13:484–497
14. Kappler S, Henning A, Kreisler B et al (2014) Photon counting CT at elevated X-ray tube currents: contrast stability, image noise and multi-energy performance. Proc SPIE Med Imaging. https://doi.org/10.1117/12.2043511
15. Bland JM, Altman D (1986) Statistical methods for assessing agreement between two methods of clinical measurement. Lancet 327:307–310
16. Schlomka JP, Roessl E, Dorscheid R et al (2008) Experimental feasibility of multi-energy photon-counting K-edge imaging in pre-clinical computed tomography. Phys Med Biol 53:4031
17. Symons R, De Bruecker Y, Roosen J et al (2018) Quarter-millimeter spectral coronary stent imaging with photon-counting CT: initial experience. J Cardiovasc Comput Tomogr. https://doi.org/10.1016/j.jcct.2018.10.008
18. Meyer M, Haubenreisser H, Schoepf UJ et al (2014) Closing in on the K edge: coronary CT angiography at 100, 80, and 70 kV—initial comparison of a second-versus a third-generation dual-source CT system. Radiology 273:373–382
19. Sandfort V, Lima JAC, Bluemke DA (2015) Noninvasive imaging of atherosclerotic plaque progression. Circ Cardiovasc Imaging 8:e003316
20. Symons R, Morris JZ, Wu CO et al (2016) Coronary CT angiography: variability of CT scanners and readers in measurement of plaque volume. Radiology 281:737–748
21. Mahesh M, Zimmerman SL, Fishman EK (2014) Radiation dose shift in relative proportion: the case of coronary artery calcium studies. J Am Coll Radiol 11:634–635
22. Gebhard C, Fiechter M, Fuchs TA et al (2013) Coronary artery calcium scoring: influence of adaptive statistical iterative reconstruction using 64-MDCT. Int J Cardiol 167:2932–2937
23. Willemink MJ, den Harder AM, Foppen W et al (2016) Finding the optimal dose reduction and iterative reconstruction level for coronary calcium scoring. J Cardiovasc Comput Tomogr 10:69–75
24. Pourmorteza A, Symons R, Schoeck F et al (2018) Dose efficiency of quarter-millimeter photon-counting CT: first-in-human results. Investig Radiol. https://doi.org/10.1097/RLI.0000000000000463
25. Symons R, Cork TE, Lakshmanan MN et al (2017) Dual-contrast agent photon-counting computed tomography of the heart: initial experience. Int J Cardiovasc Imaging. https://doi.org/10.1007/s10554-017-1104-4
26. Mannil M, Hickethier T, von Spiczak J et al (2017) Photon-counting Ct: high-resolution imaging of coronary stents. Investig Radiol 53:143–149
27. Symons R, Krauss B, Sahbaee P et al (2017) Photon-counting CT for simultaneous imaging of multiple contrast agents in the abdomen: an in vivo study. Med Phys. https://doi.org/10.1002/mp.12301
28. Muenzel D, Bar-Ness D, Roessl E et al (2016) Spectral photon-counting CT: initial experience with dual–contrast agent K-edge colonography. Radiology 283:723–728. https://doi.org/10.1148/radiol.2016160890
29. Muenzel D, Daerr H, Proksa R et al (2017) Simultaneous dual-contrast multi-phase liver imaging using spectral photon-counting computed tomography: a proof-of-concept study. Eur Radiol Exp 1:25
30. Cormode DP, Si-Mohamed S, Bar-Ness D et al (2017) Multicolor spectral photon-counting computed tomography: in vivo dual contrast imaging with a high count rate scanner. Sci Rep 7:4784
31. Dangelmaier J, Bar-Ness D, Daerr H et al (2018) Experimental feasibility of spectral photon-counting computed tomography with two contrast agents for the detection of endoleaks following endovascular aortic repair. Eur Radiol. https://doi.org/10.1007/s00330-017-5252-7